

Soot Volume Fraction and Temperature Properties of High Liquid Loading Spray Flames

R.A. Wade, Y.R. Sivathanu, and J.P. Gore
Thermal Sciences and Propulsion Center
School of Mechanical Engineering
Purdue University
West Lafayette, IN 47907

Abstract

The relationship between burning rate, visible flame length, and sooting properties of spray flames is investigated. Multiwavelength emission/absorption spectroscopy was applied to the measurement of soot volume fractions and temperatures for high liquid loading effervescent atomized flames. The statistics of the emission and absorption data were interpreted in terms of the statistics of the local properties using a novel discrete probability function based deconvolution method. The results show the coupled effects of soot volume fractions and temperature on the radiative heat loss from the spray flames. The effervescent atomized burner configuration allows a study of the radiation properties over a wider range of soot and temperature combinations than that allowed by gas jet flames. Comparison between conventional deconvolution techniques and the present method show that consideration of turbulence/ radiation interactions is essential in applying tomography to time varying fields.

Introduction

Accidental rupture of liquid storage tanks, puncture of pipelines, and oil well blowout fires may cause hazardous high liquid loading spray fires [1]. Material exiting the accidental leaks has high liquid loading with small vapor fractions. The vapor can cause atomization and vaporization of liquid fuel leading to spray flame stabilization. A full understanding of these fires will allow industrial designers to minimize the potential hazard to personnel. Dutta et.al. [2] found that these flames have not been studied extensively in the literature, but can be very important for fire safety issues. An example of these fires can be found in the work of Evans et.al. [1] who assesses the heat release rate of the crude oil well fires in Kuwait using flame height and thermal radiation measurements. The mass of lost the crude oil was sought from the measured global properties of radiative heat loss fraction and visible flame length. Enhanced understanding of spray jet flames will contribute to the assessment of economic losses and enhancement of fire safety.

The visible flame length is strongly influenced by its sooting tendency. The flame is visible primarily due to the glowing soot particles. As the concentration and temperature of the soot particles increase, the visible flame length is expected to increase. Soot concentration and temperature also strongly effect the radiative heat loss which cools the flame and decreases the visible flame length. The objective of the present paper is to report measurements of soot volume fractions and temperatures in high liquid loading spray jet fires and interpret these in terms of the visible flame length and radiative loss fraction data.

Theoretical Background

Following ref. [3], line of sight measurements of monochromatic absorption and two wavelength emission are obtained for chord-like paths at various heights in the flames. The line of sight absorption data are related to an effective soot volume fraction [4]. However, following ref. [5], these data can also be used to find local soot volume fractions.

Beer's law gives an expression for absorption soot volume fraction, f_v (ppm), when the soot particle diameters are below the Rayleigh limit.

$$f_v = \frac{-\ln\left(\frac{I_\lambda}{I_{\lambda^0}}\right) \cdot \lambda}{k_\lambda \cdot L} \quad (1)$$

The argument of the logarithm is the intensity ratio of light that passes through the medium to the incident light. This ratio is the transmittance, τ_λ . In this expression k_λ , given by eqn. (2), is the spectral extinction coefficient which is an optical property of the soot based on its refractive indices.

$$k_\lambda = \frac{36\pi \cdot n \cdot k}{(n^2 - k^2 + 2)^2 + 4n^2 \cdot k^2} \quad (2)$$

The value of k_λ for a He-Ne laser at 632 nm is 4.892 based on a soot refractive index of 1.57-0.56j. These expressions allow the measurement of soot volume fraction knowing wavelength, geometry, spectral absorption coefficient, and transmittance. The

wavelength is specified by using a laser, the geometry is determined by the experimental apparatus, the spectral absorption coefficient is calculated using eqn. (2), and the transmittance is obtained experimentally. The emission intensity leaving a volume of soot is given by:

$$I_{\lambda} e^{\left(\frac{-k_{\lambda} \cdot f_v \cdot L}{\lambda} \right)} \cdot 2 \cdot h \cdot c^2 \cdot \lambda^5 \cdot \left(e^{\frac{h \cdot c}{\lambda \cdot k_b \cdot T}} - 1 \right) \quad (3)$$

k_{λ} is the spectral absorption coefficient, L is the path length, f_v is the effective soot volume fraction based on emission, h is Planck's constant, k_b is the Boltzmann's constant, and c is the speed light in vacuum. This expression can be expanded using a two term Taylor series. Intensity is a function of wavelength for a source at a fixed temperature. The soot volume fraction and path length drop out of the expression if a ratio of these intensities is taken using the expansion. The result gives the ratio of intensities.

$$\frac{I_{\lambda 1}}{I_{\lambda 2}} = \frac{k_{\lambda 1} \cdot \lambda_2^5 \cdot e^{\frac{h \cdot c}{k_b \cdot T} \left(\frac{1}{\lambda_2} - \frac{1}{\lambda_1} \right)}}{k_{\lambda 2} \cdot \lambda_1^5} \quad (4)$$

The two wavelengths used in this study are: 900 nm and 1000 nm, where the soot spectral extinction coefficients are $k_{900}=5.288$ and $k_{1000}=5.473$. The intensities are measured experimentally and the expression is solved for the effective temperature T of the path L .

Line of sight absorption measurements are used to investigate soot volume fraction properties in the flames. These data are deconvoluted to obtain local properties. The flame is taken to consist of axisymmetric rings, with each ring having an effective soot volume fraction. As the laser passes through the flame, each ring makes a contribution to the light absorbed by the path. Local properties can be obtained using a deconvolution scheme. Path integrated values for temperature and local values for soot volume fractions obtained using a novel deconvolution procedure based on probability density functions (PDF) are reported. Local values of temperatures will be obtained in future studies.

Local properties give an enhanced understanding for the highly non-linear processes like radiative heat transfer and chemical kinetics. Deconvolution is complicated by the turbulent nature of the jet spray flames which is partly described by the PDF. Each path integrated PDF must be deconvoluted ring by ring to gain a knowledge of the local properties. The deconvolution method is called

the Abel integral method and is commonly referred to as "onion-peeling." Each ring has a characteristic PDF for transmittance. Absorption measurements over a path consisting of segments of two rings yields the product of the transmittances, $\tau_T = \tau_1 \tau_2$. The probability for a specific value of transmittance in the total path is related to the probability of each realization of the transmittance in the two rings. The transmittance is also related to the geometry of the rings. Each PDF is discretized and each bin is processed in relation to all other bins of the other discrete probability density functions [5]. The outer most chord in the flame makes the first PDF. The second chord crosses two rings from which knowledge of the total path integrated PDF and the PDF for the outer ring can be used to solve for the PDF over the inner ring. Thus PDF deconvolution works its way into the center of the flame to give local PDFs for each ring [5]. The local soot volume fraction averages are found from the local PDF.

The average transmittance for each chord-like path can be used to obtain an estimate of the local average soot volume fraction. However, this procedure results in the neglect of the effects of turbulent fluctuations on transmittance. In the present work, the errors caused by such a neglect are shown quantitatively.

Experimental Methods

High liquid loading spray jet flames with gas to liquid ratios between 0.05 and 0.25 are stabilized over an effervescent atomizer burner [2]. Toluene (C_7H_8) is used as the liquid fuel. Methane (CH_4) is used as the atomizing gas. A small hydrogen (H_2) pilot ring flame stabilizes the spray flame. The two phase flow from the atomizer is best characterized using the total combined heat release rate (Q_d) computed from the nominal heating values of 39,912 kJ/kg for toluene, 50,144 kJ/kg for methane, and 109,921 kJ/kg for hydrogen. At each heat release rate, variation of the methane to liquid mass ratio (MLR) and Hydrogen to liquid mass ratio (HLR) resulted in 19 test conditions. Five of these conditions were selected, as shown in Table 1, for measurements of soot volume fractions. The operating conditions ranged in heat release rate from 10 kW to 25 kW, MLR varying from 5% to 25% and HLR varying from 5% to 13%. This test matrix allowed a study of the influence of each parameter. Each of the five flames were studied at three representative axial locations selected to be 1/4, 1/2 and 3/4 of the visible flame length, H_f .

The experimental arrangement for the absorption and emission measurements is shown schematically in Fig. 1.

Absorption measurements require a known light intensity to be directed through the flame and detection of the resulting intensity after the flame. This is accomplished using a 5 mW He-Ne laser, a beam splitter, and laser power meters (photo diode) on either side of the flame. To minimize noise, the laser beam was chopped at 2000 Hz and the output signals were passed through a high pass filter, a lock in amplifier, and a low pass filter. A reference measurement is made without the flame to determine the incident intensity.

The temperature is determined using the emitted light intensity from the hot soot. Narrow band filters at 900 nm and 1000 nm wavelength were placed over the two photomultiplier tubes. The output signal was passed through a low pass electronic filter. The photomultiplier tubes were calibrated by sampling their output when exposed to a black body radiation source. A collimating tube was used to define the view of the photomultiplier tubes. It is important to note that the measured temperatures represent an effective average of the hot soot along the radiation path. Any cold soot in the flame and hot gases do not contribute to the emission signals at 900 and 1000 nm. When the emission signal is low the effective temperature is set to 300 K. This procedure introduces severe downward bias in the absence of soot particles.

All the signal voltage output values were sampled by a computer using a four channel A/D board sampling at 1000 Hz. Each measurement lasted 5 seconds so that the turbulent fluctuations of the flame are captured statistically. The burner was mounted on a slide for simple adjustment while the optics remained stationary. The initial position of the burner had the laser pass through the center of the flame and then the burner was radially advanced until the oscilloscope display from the photomultiplier tubes gave no signal indicating that the sooty part of the flame was no longer in the view field.

Table 1: Operation Conditions

Q_6 kW	Toluene, mg/s	MLR, %	HLR, %	H_6 cm	X_R
10	206	5	5	43	.34
10	172	5	13	45	.33
10	147	25	13	33	.11
20	413	5	5	55	.37
20	344	5	13	59	.44

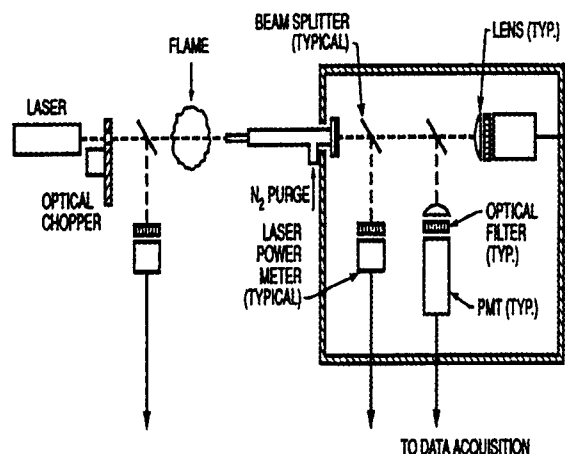


Figure 1: Experimental Setup

Results and Discussion

Flame Length and Radiative Heat Loss Fraction

The dependence of flame length on soot volume fractions and temperature is sought in this work. Fig. 2 shows that the visible flame length increases as the heat release rate increases. The flame length also increases as the methane to liquid ratio decreases. The radiative heat loss fraction, X_R , is the energy leaving the flame by radiative heat transfer normalized by the nominal heat release of the fuel. The radiative heat loss fraction was measured with a radiometer using a single point technique developed in this laboratory[6]. The results were confirmed for some flames by performing a scan of points to form a semiinfinite cylinder. The single point radiation measurements are shown in Fig. 3. For low MLRs, X_R increases and then decreases as the heat release rate is increased. For high MLRs, X_R shows a decreasing trend for all heat release rates. This variety in the X_R variation is caused by coupling between radiative heat loss and flame temperature. The 19 operating conditions demonstrate that there is a wide range of flame lengths and radiative heat loss fractions possible.

Temperature and Soot Volume Fraction Data

The first step in the process of obtaining local properties is sampling the data and creating path integrated PDFs. This was done for the five selected flames and a sample graph for a 10 kW flame at 5% MLR and 5% HLR is shown in Fig 4. Each line in the figure represents one radial position and each box represents a different axial position in the flame. The average values for each radial position in Fig 4 are shown in Fig 5.

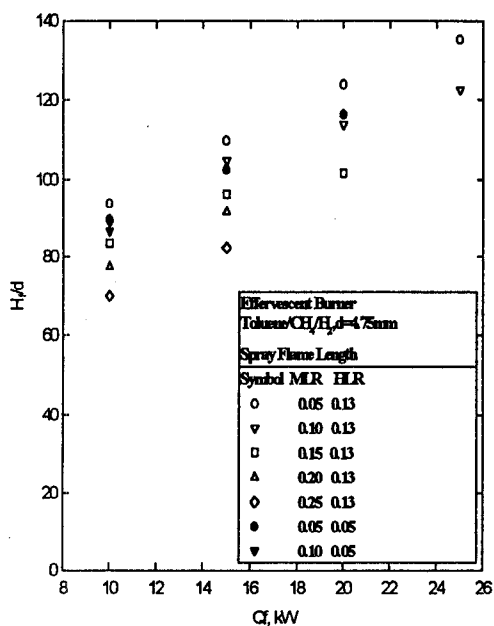


Figure 2: Visible Flame Length

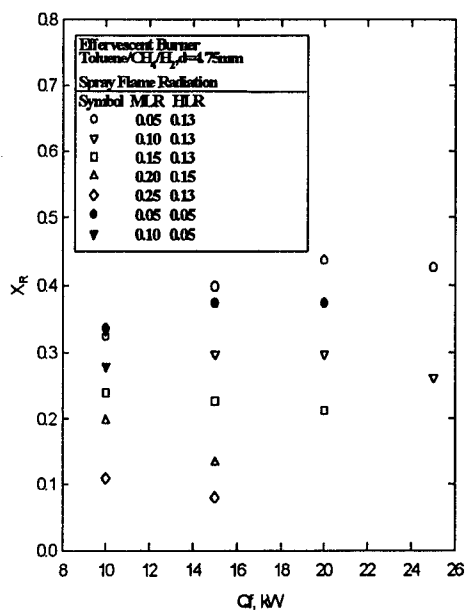


Figure 3: Radiative Fraction of Heat Release

The path averaged effective temperature data in Fig. 5 show that temperature is the highest at the diametrical chord where every ring contributes to the path integrated value. The highest temperature in the flame is 1800 K for the 0.25 H_f case. Here the transmittance is 0.8, which is above the values for

the other flames at the center. This indicates that the soot volume fractions at this location are lower but the temperatures are higher. At higher positions in the flame, the soot volume fractions increase but temperatures are lower due to radiative cooling. As expected, at higher axial positions in the flame, the transmittance and temperature profiles have a wider radial spread. The temperature of the hot soot was 1800 K at 0.25 H_f and cooling to 1500 K at 0.75 H_f . The decreasing trend in temperature with increased radial position in Fig. 5 is due to the assigned low values of 300 K being averaged with the measured temperature of the hot soot. Taking the temperature to be constant is only good as a first approximation since the radiation heat loss depends on the temperature in a nonlinear manner.

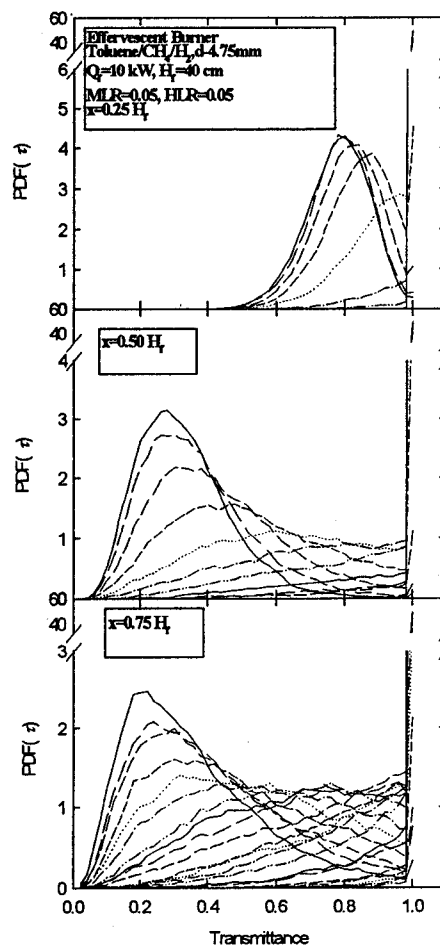


Figure 4: Path integrated PDFs

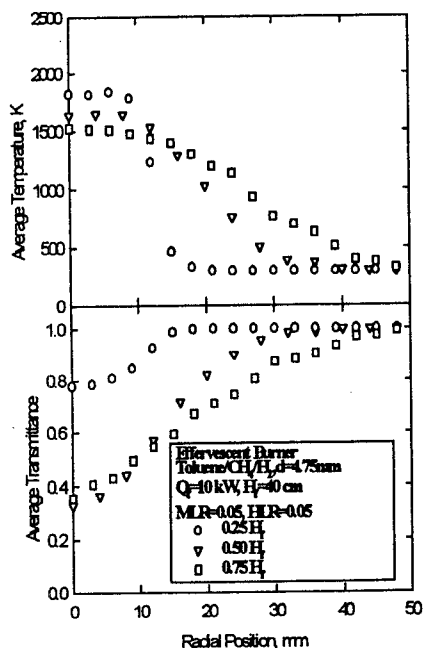


Figure 5: Path Integrated Average Values

Local soot volume fraction data are obtained using the deconvolution procedure. Path integrated values are deconvoluted to give local PDFs for transmittance as shown in Fig. 6 for the 10 kW, 5% MLR, 5% HLR flame. Each line represents a radial position and each box represents an axial position.

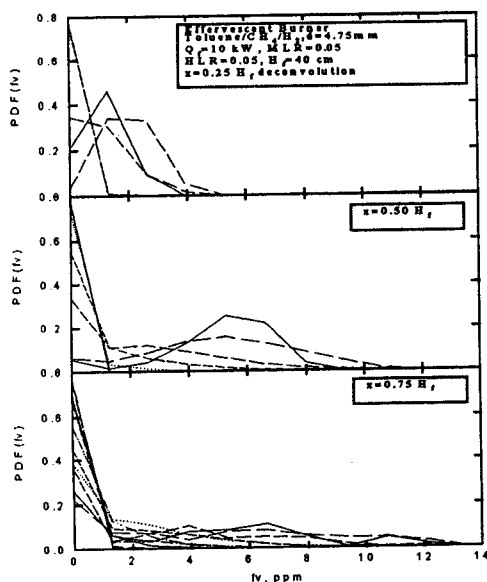


Figure 6: Local PDF of transmittance

These PDFs for each radial position in each flame can be processed to obtain graphs of the average values. This allows a simple comparison of large amounts of data. The average soot volume fractions are shown in Fig. 7 for the three 10 kW flames and Fig. 8 for the two 20 kW flames. The average results from the PDF deconvolution method are represented by filled symbols and those obtained from deconvolutions of mean transmittance are shown as open symbols.

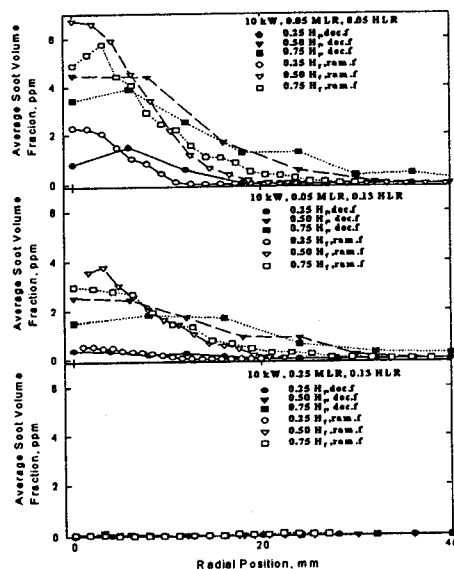


Figure 7: 10 kW Average Soot Volume Fractions

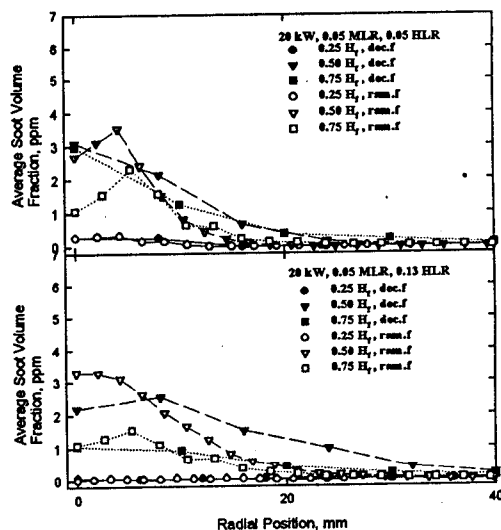


Figure 8: 20 kW Average Soot Volume Fractions

Comparing the data at the axial positions for all five flames shows that, the lowest position in the flame has the lowest volume fraction of soot. The highest volume fraction of soot occurs at half of the visible flame length. Soot volume fractions have a peak concentration for the innermost ring and drop off at farther radial positions for the 0.25 H_f flame position. For the 0.75 H_f and 0.50 H_f positions, there is a decrease in soot volume fraction at the center of the flame below the peak value which occurs at a larger radius.

The differences in the trends for the PDF deconvolution based data are primarily in the numerical values of soot volume fraction. The flame with the highest f_v is the one with 10 kW heat release and 5% MLR, 5% HLR. This flame also shows little decrease in f_v moving from 0.50 H_f to 0.75 H_f . The high f_v makes the flame visible for the longest length among the seven 10 kW flames. At 10 kW, if the MLR is increased to 25% where the flame has almost no measurable soot, the visible length is the shortest among the flames studied. In this case the absence of soot luminosity makes the flame appear shorter. The 20 kW flames have a higher radiative fraction at a higher HLR. The 13% HLR flame has a more pronounced dip in the f_v at the center but the radial distribution is wider which indicates more total soot in the flame to provide luminosity for a longer flame. However, the high amount of soot also contributes to radiative cooling so that the flame length is not significantly different than that of the flame with a lower HLR.

Comparing the PDF deconvolution results to those obtained from average transmittances shows that the effects of turbulent fluctuations are

Conclusions

Among the factors influencing visible flame lengths of high liquid loading jet fires, soot temperature and volume fractions were investigated. Path integrated values of temperature were obtained and found to be steady. Local PDFs for soot volume fractions were found from the path integrated values, and the averages were compared to a simpler technique that neglects turbulent radiation interaction. As seen from the results, consideration of these interactions is important. The significant increase in soot volume fraction explains the increase in visible flame length with decreasing MLR.

Acknowledgment

This work was funded by the Center for Fire Research, National Institute of Standards and Technology, Building and Fire Research Laboratory, Grant No. 60NANB3D1441 with Dr. David D. Evans serving as NIST technical officer.

References

1. Evans, D.D., Madrzykowski, D., and Haynes, G.A., *Fire Safety Science--Proceedings of the Fourth International Symposium*, (T. Kashiwagi, Ed.) p. 1279.
2. Dutta, P., Gore, J.P., Sivathanu, Y.R., Sojka, P.E., *Combust. Flame*. 97:251-260 (1994).
3. Sivathanu, Y.R., and Gore, J.P., *Combust. Sci. Technol.* 76:45-66 (1991).
4. Sivathanu, Y.R., Gore, J.P., Janssen, J.M., and Senser, D.W., *J. Heat Transf.* 115:653-658 (1993).
5. Sivathanu, Y.R. and Gore, J.P., *JQSRT* 50, 483 (1993).
6. Sivathanu, Y.R. and Gore, J.P., *Combust. Flame* 94:265-270 (1993).